Dalton Transactions

Accepted Manuscript

ROYAL SOCIETY OF CHEMISTRY

www.rsc.org/dalton

Cite this: DOI: 10.1039/c0xx00000x

www.rsc.org/xxxxxx

ARTICLE TYPE

Metal-organic frameworks based on [1,1':3',1''-terphenyl]-3,3'',5,5''-tetracarboxylic acid ligand: syntheses, structures and magnetic properties

Xiaofeng Lv, Lu Liu, Chao Huang, Li'an Guo, Jie Wu*, Hongwei Hou*, Yaoting Fan

Received (in XXX, XXX) Xth XXXXXXXXX 20XX, Accepted Xth XXXXXXXXX 20XX
First published on the web Xth XXXXXXXXX 20XX
DOI: 10.1039/b000000x

The solvothermal reactions of [1,1':3',1''-terphenyl]-3,3'',5,5''-tetracar-boxylic acid (H_4TPTA) with transition metal cations afford five novel coordination polymers in the presence of three pyridine ligands (4,4′-bipy = 4,4′-bipyridine, 2,2′-bipy = 2,2′-bipyridine and phen = 1,10-Phenanthroline), namely, $[M(TPTA)_{0.5}(4,4'\text{-bpy})_{0.5}(H_2O)_2]_n$ (M = Co for (**1**), Ni for (**2**)), $\{[Mn_2(TPTA)(2,2'\text{-bpy})H_2O]\cdot 1.5H_2O\}_n$ (**3**), $[M(H_2TPTA)(phen)]_n$ (M = Mn for (**4**), Co for (**5**)). Their structures have been determined by single-crystal X-ray diffraction analyses and further characterized by elemental analyses, IR spectra, powder X-ray diffraction (PXRD), and thermogravimetric (TG) analyses. Polymers **1** and **2** are isomorphous and exhibit 3D 4-fold interpenetrated networks with the point Schläfli symbol of $(4^2.10^4)$ (4.10^2). Polymer **3** shows a 2D layer framework. Polymers **4** and **5** are also isomorphous and each displays a one-dimensional (1D) chain, which further forms a 2D supramolecular architecture via inter-chain π···π interactions. Moreover, variable-temperature magnetic susceptibilities of polymers **3**–**5** exhibit overall weak antiferromagnetic coupling between the adjacent M(II) ions.

Introduction

The rational design and synthesis of functional coordination polymers has inspired a wide range of research over the past few decades due to their rich structural diversities[1] and important industrial application potentials in the areas of molecular magnetism,[2] gas storage,[3] ion exchange,[4] nonlinear optics,[5] drug delivery[6] and heterogeneous catalysis.[7] The solvothermal method has been widely used to synthesize coordination polymers since it can alleviate the problems of ligand solubility and improve the reactant reactivity during the crystallization process. In this method, the construction of coordination polymers is largely influenced by many factors such as the coordination of metal ions, the structural characteristics of multidentate organic ligands, the metal–ligand ratio, the solvent, and the temperature,[8-11] etc. Among those mentioned above, the selection of ligands is crucial in the construction of coordination polymers. Up to now, a great number of polybasic carboxylic acids ligands have been employed to assemble coordination polymers due to their rich coordination modes. In addition, carboxylate groups are good hydrogen-bond acceptors as well as donors, depending upon the degree of deprotonation.[12] In the meantime, the pyridine ligands are usually introduced into the reaction system to exchange the frameworks. The reasons can be generalized as follows: firstly, the pyridine rings could provide feasibility for lower dimensional networks to be extended into multi-dimensional ones; secondly, pyridine rings are good candidates in terms of hydrogen-bonding formation, and π–π stacking interactions that are significant for affording extended open frameworks via polymerization.[13]

Thus, these considerations inspired us to explore new coordination architectures with [1,1':3',1''-terphenyl]-3,3'',5,5''-tetracarboxylic acid (H_4TPTA) (Scheme S1) and pyridine ligands including 4,4′-bipyridine (4,4′-bipy), 2,2′-bipyridine (2,2′-bipy) and 1,10-phenanthroline. In this paper, we reported the syntheses and characterizations of five new coordination polymers, $[M(TPTA)_{0.5}(4,4'\text{-bpy})_{0.5}(H_2O)_2]_n$ (M = Co(**1**), Ni(**2**)), $\{[Mn_2(TPTA)(2,2'\text{-bipy})H_2O]\cdot 1.5H_2O\}_n$ (**3**), $[M(H_2TPTA)(phen)]_n$ (M = Mn(**4**), Co (**5**)). And then, we also reported the thermal stability and magnetic property of as-synthesized coordination polymers.

Experimental section

Materials and Synthesis.

All reagents and solvents were commercially available without any further purification, except for ligand H_4TPTA, which was synthesized according to the literature.[13g] The IR spectra were

The College of Chemistry and Molecula Engineering, Zhengzhou University, Zhengzhou 450052, P. R. China. E-mail: houhongw@zzu.edu.cn; wujie@zzu.edu.cn. *†Electronic supplementary information (ESI) available: selected bond lengths and bond angles, additional crystal figures, powder X-ray patterns for complexes **1**−**5**.CCDC reference numbers: 1009774−1009778 for **1**−**5**. For ESI and crystallographic data in CIF or other electronic format see DOI:10.1039/b000000x/*

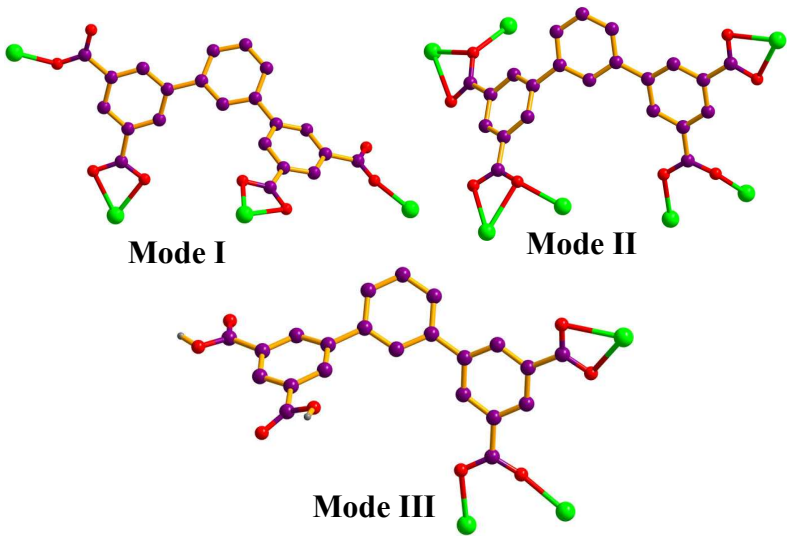

Chart 1. Different Coordination Modes of H_4TPTA in Complexes **1**–**5**.

measured on a Bruker-ALPHA spectrophotometer at the range of 400–4000 cm^{-1}. The elemental analyses(C, H, and N) were performed on a FLASH EA 1112 elemental analyzer. All the PXRD patterns were recorded on a PANalytical X'Pert PRO diffractometer with the use of Cu $K\alpha_1$ radiation. Thermogravimetric scanning calorimetry (TG) measurements were performed by heating the sample on a Netzsch STA 409PC differential thermal analyzer with a heating rate of 10 ºC min^{-1} from ambient temperature under an air atmosphere.

The synthesis of $[Co(TPTA)_{0.5}(4,4'\text{-bpy})_{0.5}(H_2O)_2]_n$ (1). A mixture of H_4TPTA (0.020 g, 0.05 mmol), 4,4′-bpy (0.0156 g, 0.1mmol), $Co(NO_3)_2{\cdot}6H_2O$ (0.0291 g, 0.1 mmol), 4 mL CH_3CN and 4 mL H_2O was sealed in a Teflon-lined stainless steel vessel and heated to 160 °C for 3 days, which was followed by slow cooling (a descent rate of 5 °C h^{-1}) to room temperature. The red block crystals of **1** were obtained. Yield of 71% (based on Co). Anal. (%) calcd for $C_{16}H_{13}NO_6Co$ (374.21): C, 51.35; H, 3.50; N, 3.74. Found: C, 51.18; H, 3.41; N, 3.49. IR (KBr pellet, cm^{-1}): 3613m, 3373s, 3127s, 1616v, 1545v, 1426v, 1404s, 1254m, 1219w, 820w, 717w, 636m, 586w.

The synthesis of $[Ni(TPTA)_{0.5}(4,4'\text{-bpy})_{0.5}(H_2O)_2]_n$ (2). A mixture of H_4TPTA (0.020 g, 0.05 mmol), 4,4′-bpy (0.0156 g, 0.1 mmol), $Ni(NO_3)_2{\cdot}6H_2O$ (0.0290 g, 0.1 mmol), 4 mL CH_3CN and 4 mL H_2O was sealed in a Teflon-lined stainless steel vessel and heated to 160 °C for 3 days, which was followed by slow cooling (a descent rate of 5 °C h^{-1}) to room temperature. The green block crystals of 2 were obtained. Yield of 63% (based on Ni). Anal. (%) calcd for $C_{16}H_{13}NO_6Ni$ (373.97): C, 51.38; H, 3.50; N, 3.75. Found: C, 50.74; H, 3.66; N, 3.42. IR (KBr pellet, cm^{-1}): IR (cm^{-1}, KBr): 3609m, 3318s, 3033w, 3128s, 1647v, 1613v, 1536v, 1401v, 771m, 722m, 638m, 593m.

The synthesis of $\{[Mn_2(TPTA)(2,2'\text{-bpy})(H_2O)]{\cdot}1.5H_2O\}_n$ (3). A mixture of H_4TPTA (0.020 g, 0.05 mmol), 2,2′-bpy (0.0156 g, 0.1 mmol), $MnCl_2{\cdot}4H_2O$ (0.0100 g, 0.05 mmol), 4 mL CH_3CN and 4 mL H_2O was sealed in a Teflon-lined stainless steel vessel and heated to 160 °C for 3 days, which was followed by slow cooling (a descent rate of 5 °C h^{-1}) to room temperature. The yellow block crystals of **3** were obtained. Yield of 54% (based on Mn). Anal. (%) calcd for $C_{32}H_{22}N_2O_{10}Mn_2$ (704.40): C, 54.56; H, 3.14; N, 3.97. Found: C, 54.58; H, 2.99; N, 4.06. IR (KBr pellet, cm^{-1}): 3426s, 3132w, 1619v, 1548v, 1396v, 1304v, 770m, 639m, 552w.

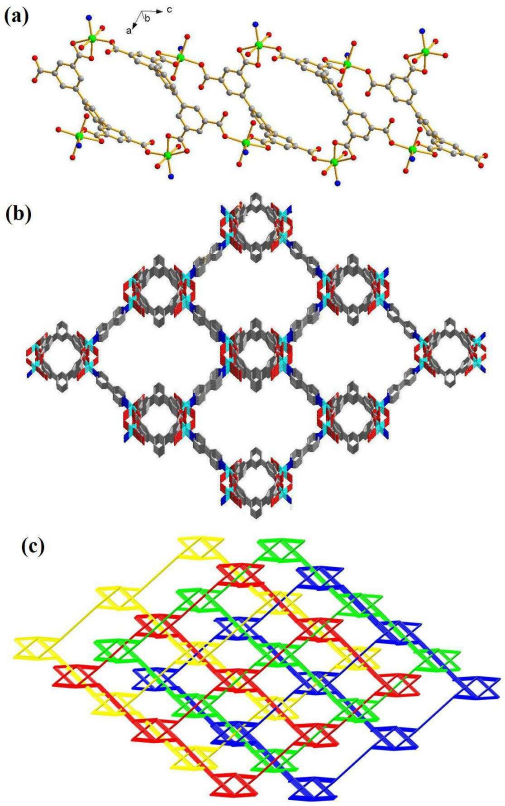

Fig.1 (a) The 1D chain linked by Co^{2+} and $TPTA^{4-}$ ions in **1**. (b) The individual 3D structure of **1**. (c) The 4-fold interpenetrated structure of **1**.

The synthesis of $[Mn(H_2TPTA)(phen)]_n$ (4). A mixture of H_4TPTA (0.020 g, 0.05 mmol,), phen (0.0198 g, 0.1 mmol), $MnCl_2·4H_2O$ (0.0100 g, 0.05 mmol), 5 mL CH_3CN and 5 mL H_2O was sealed in a in a Teflon-lined stainless steel vessel and heated to 130 °C for 3 days, which was followed by slow cooling (a descent rate of 5 °C h^{-1}) to room temperature. Yellow block crystals of **4** were obtained. Yield of 51% (based on Mn). Anal. (%) calcd for $C_{34}H_{20}N_2O_8Mn$ (639.47): C, 63.86; H, 3.15; N, 4.38. Found: C, 63.53; H, 3.08; N, 4.21. IR (KBr pellet, cm^{-1}): 3128w, 1723v, 1612v, 1540v, 1396v, 1145v, 1102v, 775m, 725m, 630w.

The synthesis of $[Co(H_2TPTA)(phen)]_n$ (5). A mixture of H_4TPTA (0.020 g, 0.05 mmol), phen (0.0198 g, 0.1 mmol), $Co(NO_3)_2·6H_2O$ (0.0291 g, 0.1 mmol), 5 mL CH_3CN and 5 mL H_2O was sealed in a in a Teflon-lined stainless steel vessel and heated to 130 °C for 3 days, which was followed by slow cooling (a descent rate of 5 °C h^{-1}) to room temperature. Red block crystals of **5** were obtained. Anal. (%) calcd for $C_{34}H_{20}N_2O_8Co$ (643.46): C, 63.46; H, 3.13; N, 4.35. Found: C, 63.27; H, 3.13; N, 4.36. IR (KBr pellet, cm^{-1}): 3126w, 1722v, 1613v, 1542v, 1396v, 1150v, 1110v, 773m, 698m, 633w.

Crystal Data Collection and Refinement.

Single X-ray diffraction measurements for polymers **1**–**5** were carried out on a Rigaku Saturn 724 CCD at 298 K, using graphite-monochromated Mo Kα radiation (λ = 0.71073 Å). The structures were solved by direct methods and refined with a fullmatrix least-squares technique based on F^2 with the SHELXL-97 crystallographic software package.[14] All non-hydrogen atoms were refined anisotropically, whereas hydrogen atoms were located and refined geometrically. The position of water molecules could not be resolved from Fourier maps in the crystal of **3.** No satisfactory disorder model could be achieved, and therefore the SQUEEZE program implemented in PLATON was used to remove these electron densities. The final chemical formula of **3** was calculated from SQUEEZE results combined with the TGA and elemental analysis data. The crystal parameters, data collection, and refinement results for all compounds are summarized in Table S1. Selected bond lengths and angles are listed in Table S2 (in the Supporting Information). Crystallographic data for **1**−**5** have been deposited at the Cambridge Crystallographic Data Centre with CCDC reference numbers 1009774−1009778.

Magnetic Susceptibility Measurements.

Variable-temperature magnetic susceptibilities of **3**−**5** were carried out on a SQUID MPMS XL-7 instrument with phase-pure crystalline samples under the applied field of 1000 Oe in the temperature region of 2−300 K. The diamagnetic corrections were conducted utilizing Pascal's constants.[15a]

Results and Discussion

Description of Crystal Structures

$[Co(TPTA)_{0.5}(4,4'\text{-bpy})_{0.5}(H_2O)_2]_n$ (1) and $[Ni(TPTA)_{0.5}(4,4'\text{-bpy})_{0.5}(H_2O)_2]$ (2). The single crystal X-ray structural analysis reveals that polymers **1** and **2** crystallize in the monoclinic space group *C*/2*c*, and they are isostructures. Therefore, polymer **1** is employed as a representative structure to be described in detail. The asymmetric unit of polymer **1** contains a divalent Co atom on the crystallographic 2-fold rotation axis, one-half of fully deprotonated TPTA, and one-half of a 4,4′-bpy. The unique Co ion maintains a distorted octahedral coordination environment and is coordinated by three carboxylate oxygen atoms from two $TPTA^{4-}$, two oxygen atoms from two water and one nitrogen atom from the 4,4′-bipy. The Co–O bond distances are in the range of 2.023–2.232 Å, and the Co–N bond distance is 2.082 Å. In polymer **1**, all the carboxyl groups of H_4TPTA ligands are deprotonated, showing two different coordination modes: μ_1-η_1:η_1-chelating coordination mode and μ_1-η^1:η^0-coordination mode, respectively (Mode I of Chart 1). The $TPTA^{4-}$ connect with four Co^{2+} ions forming an infinite chain that is arranged parallel to the *c* crystal direction (Fig. 1a). These chains are in turn linked by 4,4′-bipy, producing a 3D framework (Figure 1b). The substantial apertures (~11.2 Å× ~11.2 Å) within a single neutral network permit the interpenetration of three other identical nets, resulting in an overall 4-fold interpenetrated network in **1** (Figure 1c). From a topology view, the network of **1** can be rationalized

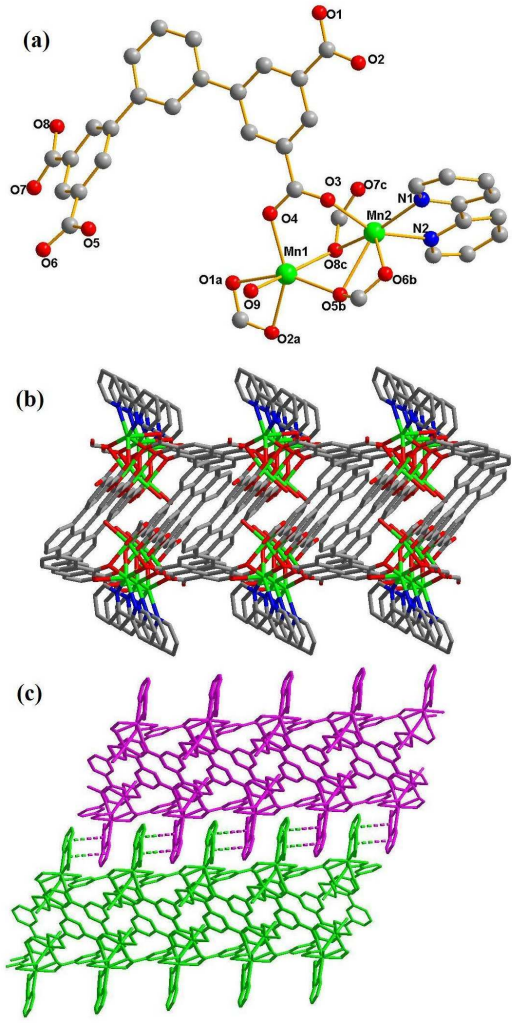

Fig 2 (a) Coordination environment of the Mn(II) ions in **3**. (b) A view of the 2D layer structure. (c) View of the 3D supramolecular structure of **3** via inter-layer π···π interactions.

to a (4,4)-connnected topology framework with point the symbol

of $(4^2{\cdot}10^4)$ $(4{\cdot}10^2)$ by denoting the Co(II) atoms to four-connected nodes and $TPTA^{4-}$ to four-connected nodes, respectively.[15b-15d] PLATON[16] analysis indicates that the effective free volume of **1** is 6.9%.

$\{[Mn_2(TPTA)(2,2'\text{-bipy})(H_2O)]\cdot 1.5H_2O\}_n$ (3). Polymer **3** crystallizes in the space group crystallizes in space group *P*-1, showing a 2D polymeric layer. The structure of **3** contains two crystallographical unique Mn(II) ions, as depicted in Fig. 2a. The Mn1 with slightly distorted octahedral coordination geometry is six-coordinated by five carboxylate oxygen atoms from four individual $TPTA^{4-}$, and one oxygen atom from the coordinated water, while the Mn2 atom adopts six-coordinated distorted octahedral geometry formed by four carboxylate oxygen atoms from three individual $TPTA^{4-}$ and two nitrogen atoms from one 2,2′-bipy. The Mn–N bond lengths fall in the range of 2.232–2.239 Å, and the Mn–O bond lengths are in the range of 2.09–2.397 Å, which is in accordance with what is reported elsewhere.[17]

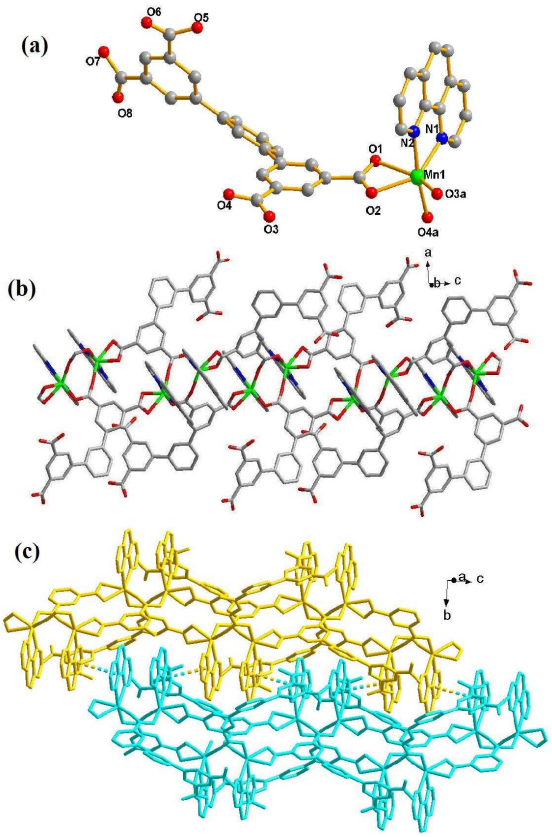

Fig. 3 (a) Coordination environment of Mn in **4**. (b) View of the 1D chain of **4**. (c) A perspective view of the 2D supramolecular layer of **4** via inter-chain π···π interactions.

The Mn1 and Mn2 centers are bridged by one bis-bidentate and two bis-tridentate carboxylate into a binuclear unit. The Mn1···Mn2 distance in the binuclear unit is 3.275Å, and the $Mn1{-}O_{carboxylate}{-}Mn2$ angles are 94.55(14), 92.77(14), respectively. The binuclear unit is further connected by $TPTA^{4-}$ (Mode II of Chart 1) to form a 2D sheet structure (Figure 2b). Furthermore, neighboring layers stack in a parallel fashion along the *a* crystal direction giving rise to a 3D supramolecular framework via inter-layer π···π interactions between 2,2′-bpy.

$[Mn(H_2TPTA)(phen)]_n$ (4) and $[Co(H_2TPTA)(phen)]_n$ (5). When a similar pyridine ligand phen, instead of 2,2′-bipy, was used into the synthetic procedure, we got a different 2D supramolecular architecture. The single-crystal X-ray diffraction analysis reveals that polymers **4** and **5** are also isostructures and crystallize in the monoclinic system, *C*2/*c* space group. Herein only the structure of **4** will be discussed as a representation. The asymmetric unit of polymer **4** contains one Mn(II) ion, one partly deprotonated H_2TPTA^{2-} and one phen. The Mn(II) center locates in a distorted octahedral geometry, coordinated by two N atoms from one chelating phen, and four carboxylate oxygen atoms from three different H_2TPTA^{2-} (Fig 3a). The Mn–N bond lengths are 2.267(3) and 2.224(2) Å, respectively, and the Mn–O bond lengths are in the range of 2.108–2.363Å.

In polymer **4**, only two carboxyl groups of the H_4TPTA are completely deprotonated (Mode III of Chart 1). The H_4TPTA acts as a μ_3-bridge linking two Mn(II) centers via one μ_1-η^1:η^1-chelating coordination mode carboxylate group and one μ_2- η^1:η^1-bridging mode carboxylate group into a one-dimensional (1D) double chain along the *c* axis. The polymer displays centro-symmetric 8- and 16-membered rings with metal-metal separations of 3.843 and 7.390 Å, respectively (Figure 3b). The terminal phen decorate the chain alternately in an outward fashion along two sides (Fig. 3b). Additional investigation of this structure indicates that interchain π···π interactions exist between these phen, with the centroid–centroid distances of 3.699 Å. Such contacts link 1D chain into a 2D layer structure (Fig. 3c).

X-ray Power Diffraction (PXRD) Analyses and Thermogravimetric (TGA) Analyses.

Powder X-ray diffraction has been used to confirm that the crystal structures are truly representative of the bulk samples in the solid state. For **1**–**5**, the measured PXRD patterns closely match the simulated one based on the single-crystal X-ray data, indicative of pure products (Fig. S2)

TGA was carried out to examine the thermal stability of **1**–**5** in the temperature range of 30–800 °C. As shown in Fig. 4, the TG curve of **1** shows the first weight loss of 9.64% ranging from 140 to 200 °C, which can be ascribed to the removal of two coordinated water molecules (calc. 9.62%). With temperature increasing, it began to decompose at 360 °C. Polymer **2** lost the weight of 9.2% ranging from 180 to 260 °C, which can be attributed to the removal of coordinated water molecules (calc. 9.6%). The departure of the organic components occurred at 380 °C, giving final metal oxides. The TG curve of **3** shows the mass loss of 6.09% from 112 to 358 °C, which may be due to the release of one coordinated water molecule and one and a half lattice water molecules (calcd 6.30%). Polymer **4** began to decompose when the temperature was raised up to 340 °C, while **5** began to decompose at 440 °C.

Magnetic Property.

The magnetic properties of **3**–**5** were investigated over the temperature range 2–300K. The $\chi_m T$ value of polymer **3** at 300 K is 8.15 cm^3 K mol^{-1}, which is lower than the expected value (8.75 cm^3 K mol^{-1}) of two uncorrelated spins of Mn(II) ions (S = 5/2) based on g = 2.0. With the temperature decreases, the value of $\chi_m T$ decreases continuously to 0.47 cm^3 K mol^{-1} at 2 K (Fig 5a). The plot of χ_m^{-1} versus T for **3** is consistent with the Curie–Weiss

law in the temperature range of 20–300 K, with C = 8.54 cm^3 K mol^{-1} and θ = –13.67K.

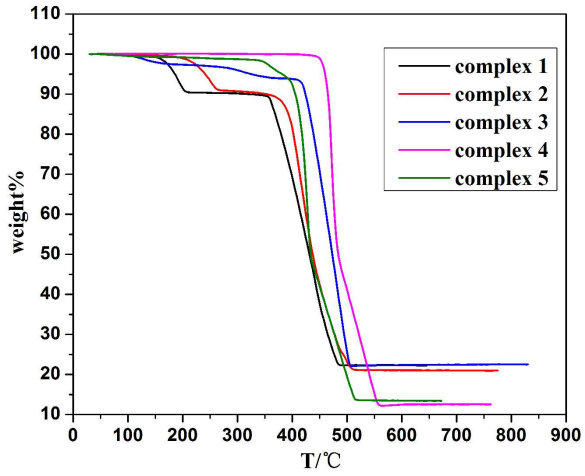

Fig.4 TGA curves of polymers **1–5**

Because the structure of polymer **3** consists of Mn(II) dimer subunits, the magnetic data were analyzed through the expression for a dinuclear Mn(II) system derived from the isotropic spin Hamiltonian $H = -2JS_1S_2$ with the interaction between adjacent dinuclear units considered[18].

$$\chi_{dimer} = \frac{2Ng^2\beta^2}{3kT} \times \frac{\sum_T S_T(S_T+1)(2S_T+1)e^{-E(S_T)/kT}}{\sum_s (2S_T+1)e^{-E(S_T)/kT}}$$

$$\chi = \frac{\chi_{dimer}}{1-\left(2zJ'/Ng^2\beta^2\right)\chi_{dimer}}$$

The best fitting parameters are J = –1.13 cm^{-1}, zJ' = –0.09 cm^{-1}, g = 1.97, and R = 2.17 ×10^{-5}. These results support operation of a weak intradimer antiferromagnetic interaction and very weak inter-dimer interaction in **3**.

The χ_mT value of **4** at 300 K is 9.41 cm^3 K mol^{-1}, which is close to the expected value (8.75 cm^3 K mol^{-1}) of two uncorrelated spins of Mn(II) ions (S = 5/2, g = 2.0). As T decreases, the value of χ_mT decreases continuously to 4.05 cm^3 K mol^{-1} at 2 K (Fig. 5b). The plot of χ_m^{-1} versus T for **4** is consistent with the Curie–Weiss law in the temperature range of 2–300 K, with C = 9.39 cm^3 K mol^{-1} and θ = –2.17 K.

Although the structure is one-dimensional chain, it can be considered as a dinuclear entity in which two Mn(II) ions are linked by two distorted *syn-syn* carboxylate bridges.[19] So the magnetic behaviour of **4** is also simulated with the same equation like **3**, and the best fitting parameters are J = –0.15 cm^{-1}, zJ' = –0.02 cm^{-1}, g = 2.06, and R = 1.46 ×10^{-5}. These negative J and θ values indicated weak intra-dimer antiferromagnetic interactions between Mn(II) ions and the inter- dimer interaction is very weak in **4**.

The magnetic interactions in the polymers **3** and **4** are weak antiferromagnetic coupling interactions. The magnetic exchange pathway in **3** is the exchange between dimeric Mn(II) ions to the carboxyl bridge (Mn-OCO-Mn) and μ_2-$O_{carboxyl}$ bridge with the superexchange angle Mn-$O_{carboxyl}$-Mn of 94.55(14), 92.77(14), respectively, while the magnetic exchange pathway in **4** only is the exchange between dimeric Mn(II) ions to the carboxyl bridge (Mn-OCO-Mn). According to some articles recorded,[20] the magnetic interaction of **3** is stronger than **4**, and the $|J|$ value of **3** is larger than **4**, which has been confirmed above.

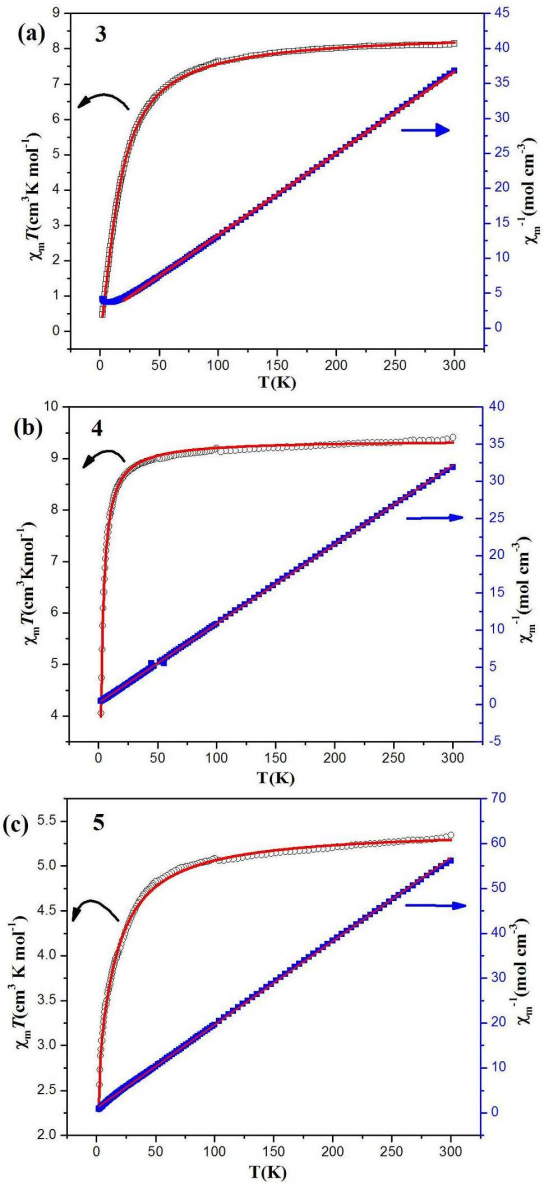

Fig.5 The χ_mT *vs* T plot and χ_m^{-1} *vs* T plot for polymers **3–5** (color symbols: experimental data; solid lines: fitting results).

For polymer **5**, the measured χ_mT value at 300 K equals 5.34 cm^3 K mol^{-1}, which is significantly larger than the spin only value of 3.75 cm^3 K mol^{-1} for two uncoupled spins Co(II) ions (g = 2.0 and S = 3/2). Upon lowering the temperature, χ_mT continuously decreases and reaches a minimum of 2.29 cm^3 K mol^{-1} at 2 K. The feature might be caused by antiferromagnetic exchange interactions as well as the effect of spin-orbit coupling. The plot of χ_m^{-1} versus T for **5** is consistent with the Curie–Weiss law in the temperature range of 2–300 K, with C = 5.37cm^3 K mol^{-1} and θ = –5.63K. In this case, in order to obtain an estimate of the strength of the antiferromagnetic exchange interaction, a simple phenomenological equation was carried out.[21]

$\chi_mT = A\exp(-E_1/kT) + B\exp(-E_2/kT)$

In this equation, $A + B$ equals the Curie constant, and E_1 and E_2

stand for the activation energies corresponding to the spin-orbit coupling and the antiferromagnetic exchange interaction, respectively.

The best fit of the experimental data gives that A + B = 5.41 cm^3 K mol^{-1}, E_1/k = 20.93K, $-E_2/k$ = –0.92 K and R = 3.88 $\times 10^{-5}$ respectively. According to the Ising chain approximation [$\chi_m T \propto \exp(+J/2kT)$], the exchange interaction J is $-1.28 cm^{-1}$, and the value induces that the antiferromagnetic exchange interaction is very weak.

Conclusions

In summary, five new coordination polymers based on [1,1':3',1"-Terphenyl]-3,3",5,5"-tetracarboxylic acid (H_4TPTA) and three pyridine ligands (4,4′-bipy, 2,2′-bipy and phen) have been synthesized. The structural diversities indicate that the pyridine ligands have influence in modulating the formation of the structures of these crystalline materials. Variable-temperature magnetic susceptibility measurements exhibit antiferromagnetic interactions between M(II) ions for polymers **3**, **4** and **5**.

Acknowledgments

This work was funded by the National Natural Science Foundation (Nos 21371155 and 21201152) and Research Fund for the Doctoral Program of Higher Education of China (20124101110002).

References

1. (a) M. O'Keeffe and O. M. Yaghi, *Chem. Rev.*, 2012, **112**, 675; (b) A. Schoedel, W. Boyette, L. Wojtas, M. Eddaoudi and M. J. Zaworotko, *J. Am. Chem. Soc.*, 2013, **135**, 14016; (c) M. Ahmad, R. Das, P. Lama, P. Poddar, P. K. Bharadwaj, *Cryst. Growth Des.,* 2012, **12**, 4624; (d) D. Frahm, F. Hoffmann, and M. Fröba, *Cryst. Growth Des*. 2014, **14**, 1719.

2. (a) X. Y. Wang, Z. M. Wang and S. Gao, *Chem. Commun.*, 2008, 281; (b) M. Kurmoo, *Chem. Soc. Rev.*, 2009, **38**, 1353; (c) X. Y. Wang, L. Wang, Z. M. Wang, S. Gao, *J. Am. Chem. Soc.,* 2006, **128**, 674; (d) S. Wöhlert, M. Wriedt, T. Fic, Z. Tomkowicz, W. Haase, and Christian Näther, *Inorg. Chem.* 2013, **52**, 1061;

3 (a) J. B. Lin, W. Xue, J. P. Zhang and X. M. Chen, *Chem. Commun.*, 2011, **47**, 926; (b) X. J. Wang, P. Z. Li, L. Liu, Q. Zhang, P. Borah, J. D. Wong, X. X. Chan, G. Rakesh, Y. X. Li and Y.L. Zhao, *Chem. Commun.*, 2012, **48**, 10286; (c) L. Qin, Z. M. Ju, Z. J. Wang, F. D. Meng, H. G. Zheng, and J.X. Chen, *Cryst. Growth Des*. 2014, **14**, 2742;

4. (a) W Meng, H. J Li, Z. Q. Xu, S. S Du, Y. X. Li, Y. Y. Zhu, Y. Han, H. W. Hou, Y. T. Fan, and M. S. Tang, *Chem. Eur. J.*, 2014, **20**, 2945; (b) R. X. Yao, X. Xu and X. M. Zhang, *Chem. Mater.*, 2012, **24**, 303; (c) S. A. Dalrymple and G. K. H. Shimizu, *Chem. Eur. J.*, 2002, **8**, 3010.

5. (a) H. W. Hou, Y. L. Wei, Y. L. Song, L. W. Mi, M. S. Tang, L.K. Li and Y. T. Fan. *Angew Chem Int Ed*, 2005, **44**: 6067; (b) H. W. Hou, Y. L. Wei, Y. L. Song, Y. T. Fan and Y. Zhu, *Inorg. Chem.*, 2004,**43**, 1323; (c) G. Li, Y. L. Song, H. W. Hou, L.K. Li, Y. T. Fan, Y. Zhu, X. R. Ming and L. W. Mi, *Inorg. Chem.*, 2003, **42**, 913

6. (a) P. Horcajada, C. Serre, M Vallet-Regí, M. Sebban, F. Taulelle, and G Férey, *Angew. Chem. Int. Ed.* 2006, **45**, 5974; (b) P. Horcajada, C. Serre, G. Maurin, N. A. Ramsahye, F. Balas, M. Vallet-Regí, M. Sebban, F. Taulelle, and G. Férey, *J. Am. Chem. Soc.*, 2008, **130**, 6774. (c) P. Horcajada, R. Gref, T. Baati, P. K. Allan, G. Maurin, P. Couvreur, G. Férey, R. E. Morris and C. Serre, *Chem. Rev.*, 2012, **112**, 1232.

7. (a) S. L. Huang, L. H. Weng and G. X. Jin, *Dalton Trans.*, 2012, **41**, 11657 (b) G. Q. Kong, S. Ou, C. Zou and C. D. Wu, *J. Am. Chem. Soc.*, 2012, **134**, 19851; (c) M. Yoon, R. Srirambalaji and K. Kim *Chem. Rev.*, 2012, **112**, 1196;(d) S. L. Huang, A. Q. Jia and G. X. Jin *Chem. Commun.,* 2013, **49**, 2403.

8. (a) N. N. Adarsh, P. Dastidar, *Cryst. Growth Des.,* 2010, **10**, 483; (b) L. Hou, W. J. Shi, Y. Y. Wang, B. Liu, W. H. Huang, Q. Z. Shi, *CrystEngComm.,* 2010, **12**, 4365; (c) L. Liu, C. Huang, Z. C. Wang, D. Q. Wu, H. W. Hou, Y. T. Fan, *CrystEngComm,* 2013, **15**, 7095; (d) Z. H. Zhang, S. C. Chen, J. L. Mi, M. Y. He, Q. Chen, M. Du, *Chem. Commun.,* 2010, **46**, 8427; (e) G. Yuan, C. Zhu, Y. Liu, W. Xuan, Y. Cui, *J. Am. Chem. Soc*., 2009, **131**, 10452; (f) G. Yuan, C. Zhu, Y. Liu, Y. Cui, *Chem. Commun.,* 2011, **47**, 3180-3182.

9. (a) Y. P. Wu, D. S. Li, F. Fu, W. W. Dong, J. Zhao, K. Zou, Y. Y. Wang, *Cryst. Growth Des.,* 2011, **11**, 3850; (b) X. J. Luan, X. H. Cai, Y. Y. Wang, D. S. Li, C. J. Wang, P. Liu, H. M. Hu, Q. Z. Shi, S. M. Peng, *Chem.-Eur. J*., 2006, **12**, 6281; (c) P. P. Liu, A. L. Cheng, Q. Yue, N. Liu, W. W. Sun, E. Q. Gao, *Cryst. Growth Des*., 2008, **8**, 1668; (d) L. Liu, J. Ding, C. Huang, M. Li, H. W. Hou, Y. T. Fan, *Cryst. Growth Des.* 2014, **14**, 3035; (e) L. Carlucci, G. Ciani, S. Maggini, D. Proserpio, M. *Cryst. Growth Des.,* 2008, **8**, 162.

10 (a) W. H. Zhang, Y. L. Song, Y. Zhang, J. P. Lang, *Cryst. Growth Des.,* 2008, **8**, 253; (*b*) L. Qin, Z. J. Wang, T. Wang, H. G. Zheng and J. X. Chen, *Dalton Trans.*, 2014, **43**, 12528; (*c*) X. Chen, S. B. Qiao, D. Liu, J. P. Lang, Y. Zhang, C. Xua and S. L. Ma; *CrystEngComm*, 2010, **12**, 1610; (d) L. Liu, X. L. Li, C. Y. Xu, G. Han, Y. Zhao, H. W. Hou, Y. T. Fan, *Inorg. Chim. Acta.* 2012, **391**, 66; (*e*) M. F. Wang, X. J. Hong, Q. G. Zhan, H. G. Jin, Y. T. Liu, Z. P. Zheng, S. H. Xu, Y. P. Cai, *Dalton Trans.,* 2012, **41**, 11898.

11 (a) J. Zhang and X. H. Bu, *Chem. Commun.*, 2008, 444; (b) S. Bauer and N. Stock, *Angew. Chem. Int. Ed.*, 2007, **46**, 6857; (c) L. L. Liu, Z. G. Ren, L. W. Zhu, H. F. Wang, W. Y. Yan, and J. P Lang, *Cryst. Growth Des*. 2011, **11**, 3479; (d) L. Liu, Y. H. Liu, G. Han, D. Q. Wu, H. W. Hou, Y. T. Fan, *Inorg. Chim. Acta.* 2013, **403**, 25.

12 (a) M. A. Nadeem, M. Bhadbhade and J. A. Stride, *Dalton Trans.*, 2010, **39**, 9860; (b) S. Q. Ma, J. P. Simmons, D. F. Sun, D. Q. Yuan and H. C. Zhou, *Inorg. Chem.*, 2009, **48**, 5263; (c) L. M. Fan, X. T. Zhang, W. Zhang, Y. S Ding, W. L. Fan, L. M. Sun, Y. Pang and X. Zhao, *Dalton Trans*., 2014, **43**, 6701; (d) P. C. Guo, T. Y. Chen, X. M. Ren, C. Xiao and W. Q. Jin, *Dalton Trans.*, 2014, **43**, 6720; (e) X. T. Zhang, L. M. Fan, X. Zhao, D. Sun, D. C. Li and J. M. Dou, *CrystEngComm*, 2012, **14**, 2053.

13 (a) F. L. Hu, S. L. Wang, B. Wu, H. Yu, F. Wang and J. P. Lang, *CrystEngComm*, 2014, **16**, 6354; (b) A. X. Tian, J. Ying, J. Peng, J. Q. Sha, Z. G. Han, J. F. Ma, Z. M. Su, N. H. Hu and H. Q. Jia, *Inorg. Chem.*, 2008, **47**, 3274; (c) H. Fu, Y. Lu, Z. L. Wang, C. Liang, Z. M. Zhang and E. B. Wang, *Dalton Trans.*, 2012, **41**, 4084; (d) Y. H. Luo, F. X. Yue, X. Y. Yu, L. L. Gu, H. Zhang and X. Chen, *CrystEngComm*, 2013, **15**, 8116; (e) H. Chen, D. Xiao, J. He, Z. Li, G. Zhang, D. Sun, R. Yuan, E. Wang and Q. L. Luo, *CrystEngComm*, 2011, **13**, 4988; (f) L. R. Yang, H. M. Zhang, Q. Q. You, L. Z. Wu, L. Liu and S. Song, *CrystEngComm*, 2013, **15**, 7505; (g) Y. Y, Liu, J. R. Li, W. M. Verdegaal, T. F. Liu and H. C. Zhou, *Chem.–Eur. J.,* 2013, **19**, 5637.

14 G. M. Sheldrick, SHELXL-97, *program for the refinement of the crystal structures*. University of Göttingen, Germany, 1997.

15 (a) E. König, *Magnetic Properties of Coordination and Organometallic Transition Metal Compounds*; Springer: Berlin, 1966; (b) The network topology was evaluated by the program "TOPOS-4.0", see: http://www.topos.ssu.samara.ru. V. A. Blatov, *IUCr CompComm. Newsl.* 2006, **7**, 4; (c) V. A. Blatov, A. P. Shevchenko, V. N. Serezhkin, *J. Appl. Crystallogr.* 2000, **33**, 1193; (d) V. A. Blatov, M. O'Keeffe, D. M. Proserpio, *CrystEngComm.* 2010, **12**, 44.

16 A. L. Spek, *J. Appl. Crystallogr.*, 2003, **36**, 7.

17 (a) Y. Y. Liu, H. J. Li, Y. X. F. Lv, H. W. Hou and Y. T. Fan, *Cryst. Growth Des.*, 2012, **12**, 3505; (b) G. X. Liu, X. C. Cha, X. L. Li, C. Y. Zhang, Y. Wang, S. Nishihara and X. M. Ren, *Inorg. Chem. Commun.,* 2011, **14**, 867; (c) L. R Yang, H. M. Zhang, Q. Q. You, L. Z. Wu, L. Liu and S. Song, *CrystEngComm*, 2013, **15**, 7505.

18. O. Kahn, *Molecular Magnetism*, VCH, New York, 1993.

19 (a) S. Konar, S. C. Manna, E. Zangrando, T. Mallah, J. Ribas, and N. R. Chaudhuri, *Eur. J. Inorg. Chem.* 2004, 4202. (b) W. E. Hatfield, *The Theory and Applications of Molecular Paramagnetism* (Eds.: E.

A. Boudreaux, L. N. Mulay), John Wiley and Sons, Inc., New York, 1976, chapter 6.

20 O. Fabelo, L. Cañadillas-Delgado, J. Pasán, F. S. Delgado, F. Lloret, J. Cano, M. Julve, and Catalina Ruiz-Pérez, *Inorg. Chem.*, 2009, **48**, 11342.

21 (a) J. M. Rueff, N. Masciocchi, P. Rabu and A. Sironi, *Eur. J. Inorg. Chem*. 2001, 2843; (b) X. Y. Wang and S. C. Sevov, *Inorg. Chem.*, 2008, **47**, 1037. (c) L. L Liang, S. B. Ren, J.Wang, J. Zhang, Y. Z. Li, H. B. Du and X. Z. You, *CrystEngComm*, 2010, **12**, 2669.

For Table of Contents Use Only

Metal-organic frameworks based on [1,1':3',1''-terphenyl]-3,3'',5,5''-tetracarboxylic acid ligand: syntheses, structures and magnetic properties

Xiaofeng Lv, Lu Liu, Chao Huang, Li'an Guo, Jie Wu*, Hongwei Hou*, Yaoting Fan

Five coordination polymers containing transition metals (Mn, Co, Ni) and organic ligand [1,1':3',1''-terphenyl]-3,3'',5,5''-tetracarboxylic acid (H_4TPTA) were synthesized and characterized. Moreover, the magnetism of the complexes **3**–**5** was also discussed.